



# Structural Insights into the Lipopolysaccharide Transport (Lpt) System as a Novel Antibiotic Target

Yurim Yoon<sup>1</sup> · Saemee Song<sup>1</sup>

Received: 19 March 2024 / Revised: 15 April 2024 / Accepted: 15 April 2024 / Published online: 31 May 2024  
© The Author(s), under exclusive licence to Microbiological Society of Korea 2024

## Abstract

Lipopolysaccharide (LPS) is a critical component of the extracellular leaflet within the bacterial outer membrane, forming an effective physical barrier against environmental threats in Gram-negative bacteria. After LPS is synthesized and matured in the bacterial cytoplasm and the inner membrane (IM), LPS is inserted into the outer membrane (OM) through the ATP-driven LPS transport (Lpt) pathway, which is an energy-intensive process. A trans-envelope complex that contains seven Lpt proteins (LptA–LptG) is crucial for extracting LPS from the IM and transporting it across the periplasm to the OM. The last step in LPS transport involves the mediation of the LptDE complex, facilitating the insertion of LPS into the outer leaflet of the OM. As the Lpt system plays an essential role in maintaining the impermeability of the OM via LPS decoration, the interactions between these interconnected subunits, which are meticulously regulated, may be potential targets for the development of new antibiotics to combat multidrug-resistant Gram-negative bacteria. In this review, we aimed to provide an overview of current research concerning the structural interactions within the Lpt system and their implications to clarify the function and regulation of LPS transport in the overall process of OM biogenesis. Additionally, we explored studies on the development of therapeutic inhibitors of LPS transport, the factors that limit success, and future prospects.

**Keywords** Lipopolysaccharide · LPS transport (Lpt) system · Antibiotics · Outermembrane biogenesis · Gram-negative bacteria

## Introduction

The emergence of drug-resistant Gram-negative bacterial strains has caused significant clinical problems because few antibiotics can treat bacterial infections by these strains (Magill et al., 2014; Willyard, 2017; Zhang et al., 2011). These bacteria produce dual membranes with distinct permeation properties that prevent many antibiotics from entering cells. While the inner membrane (IM) adopts the typical structure of a phospholipid bilayer, the outer leaflet of the outer membrane (OM) almost entirely contains amphipathic lipopolysaccharide (LPS). The peculiar permeability barrier properties of the OM result from the presence of the LPS layer in its outer leaflet (Raetz & Whitfield, 2002). Thus, interference with the biosynthesis of LPS induces membrane

instability, heightening susceptibility to antibiotics, and, in severe cases, culminates in cell death (Raetz & Whitfield, 2002; Raetz et al., 2007).

Although LPS is a diverse biomolecule with considerable species-to-species chemical variation (Zhou & Zhao, 2017), the LPS molecule generally contains the following components: a lipid A domain, which is a disaccharide backbone attached to numerous fatty acid chains; a branched nine/ten-sugar core oligosaccharide domain; and a polysaccharide chain covalently attached to the core domain, termed the O antigen (Caroff & Novikov, 2020; Raetz & Whitfield, 2002; Raetz et al., 2007). Following its independent synthesis in the cytoplasm and subsequent transport to the periplasmic side of the IM, the O antigen is connected to the lipid A-core domain by the O antigen ligase, WaaL (Ashraf et al., 2022). The lipid A-core domain is synthesized on the cytoplasmic side of the IM, while LPS maturation occurs on the periplasmic side of the IM. This transition of the lipid A-core across the IM is facilitated by the indispensable transporter MsbA (Doerrler et al., 2004; Mi et al., 2017; Raetz & Whitfield, 2002). Following the action of two enzymes, MsbA, which

✉ Saemee Song  
saemee@kriict.re.kr

<sup>1</sup> Infectious Diseases Therapeutic Research Center, Korea Research Institute of Chemical Technology, Daejeon 34114, Republic of Korea

flips nascent LPS across the IM, and WaaL, which ligates the O antigen to the nascent LPS, mature LPS is subsequently translocated from the IM to the OM; this process necessitates the involvement of seven LPS transport (Lpt) proteins, LptA–LptG, which collectively form a trans-envelope complex. An ATP-binding cassette (ABC) transporter, LptB2FG, facilitates the extraction of mature LPS from the IM and promotes its unidirectional transport through a physically interconnected bridge formed by LptC, LptA, and LptD–LptE (Narita & Tokuda, 2009; Okuda et al., 2016; Sherman et al., 2018) (Fig. 1). The LptB2FG tetramer extrudes the mature LPS from the outer leaflet of the IM and provides the energy to drive LPS transport through an ATPase-dependent mechanism. LptB2FG forms a tight complex with bitopic LptC, which is composed of a single N-terminal transmembrane (TM) helix and a periplasmic  $\beta$ -jellyroll domain (Owens et al., 2019). The N-terminal and C-terminal regions of LptC

interact with LptB2FG and LptA, respectively. Thus, LptC performs dual functions within the transporter by governing ATPase activity and serving as the binding site for the periplasmic protein LptA at the membrane (Li et al., 2019; Okuda et al., 2012; Sperandio et al., 2011). The transfer of LPS molecules from LptB2FG to LptA via LptC is another discrete ATP-dependent process in the LPS transport stage (Suits et al., 2008). According to its crystal structure (Bos et al., 2004), LptA is tetrameric and arranged end-to-end. These LptA molecules create a physical bridge that directly links LptC in the IM to LptDE in the OM. During the translocation of LPS to the OM, LPS moves along this LptA bridge, although the specific interactions between LPS and LptA remain unclear. Finally, LPS export from the LptA bridge to the outermost leaflet of the OM is performed by the  $\beta$ -barrel protein LptD and the lipoprotein LptE translocon complex (Dong et al., 2014; Freinkman et al., 2011;

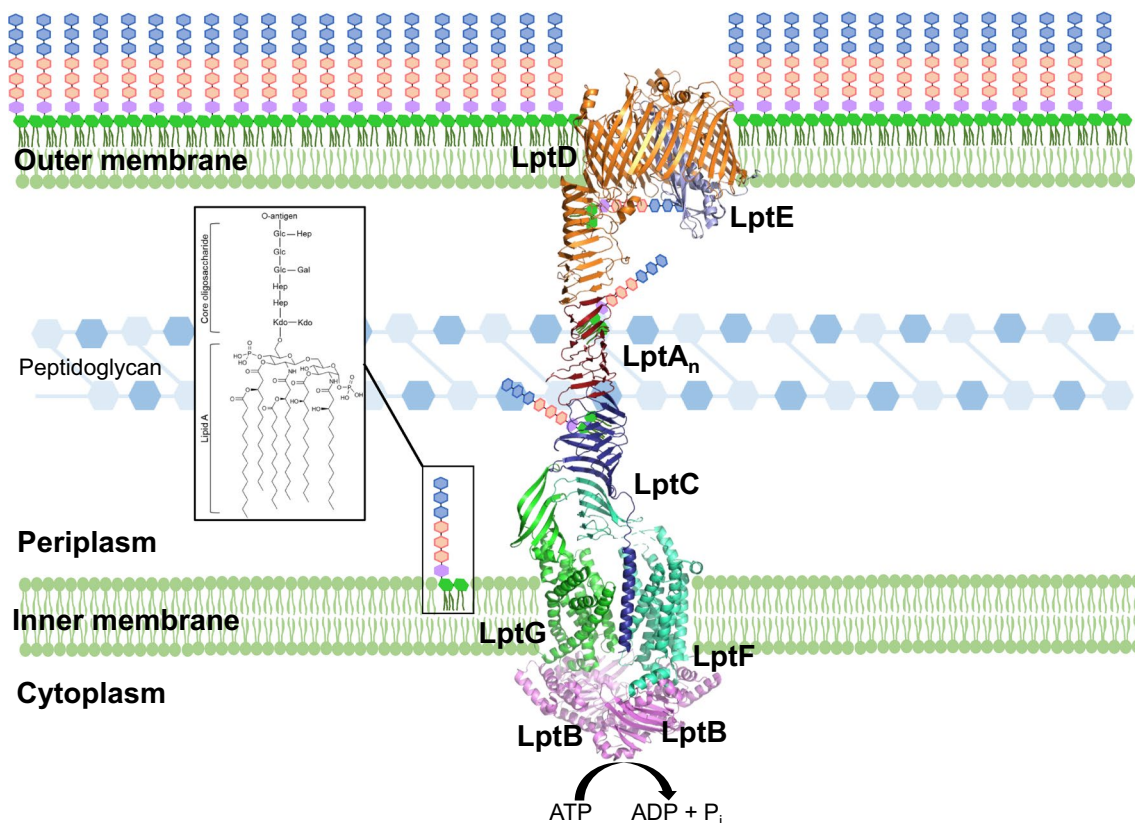


**Fig. 1** The LPS transport pathway in Gram-negative bacteria via the Lpt (lipopolysaccharide transport) machinery. The Lpt system forms a continuous protein bridge spanning the inner membrane (IM), periplasm, and outer membrane (OM). LptB (violet), LptG (green), and LptF (green-cyan) orchestrate the extraction of LPS from the inner leaflet of the IM through an ATPase-dependent mechanism (PDB: 6MJF). LPS travels through the periplasm via a unified hydrophobic groove crafted by LptC (deep blue, PDB: 3MY2), LptA (brick, PDB: 2R1A), and LptD (orange, PDB: 4Q35). LptD and LptE (light blue, PDB: 4Q35) facilitate the trans-

port of LPS to the outer leaflet of the OM. In the trigonal crystal structure (PDB: 2R1A), two LptA molecules were substituted with the C-terminal domain of LptC and the N-terminal domain of LptD. The exact number of LptA molecules within the bridge remains unknown. The representation of *E. coli* LPS encompasses only the lipid A-core moiety, omitting the O-antigen repeat moiety. Gal (D-galactose), Glc (D-glucose), Hep (L-glycerol-D-mannoheptose), and Kdo (3-deoxy-D-manno-octulosonic acid) are the components depicted. "n" denotes the number of LptA monomers

Wu et al., 2006). The N-terminus of LptD interacts with the C-terminus of LptA in a conserved manner, including the edges of the  $\beta$ -jellyroll structure, and the C-terminus of LptD forms a robust interaction with LptE, adopting a plug-and-barrel conformation (Gu et al., 2015). The lumen of the crenellated  $\beta$ -barrel structure of LptD is large enough to transport mature LPS molecules across the cell surface; then, LPS molecules exit the lateral opening of the LptDE translocon complex and are embedded in the outermost leaflet of the OM (Li et al., 2015; Romano & Hung, 2023). The PEZ model was proposed to describe the entire LPS transport pathway through the Lpt machinery, suggesting that LPS transport occurs in a similar manner to PEZ candy dispensers, in which a spring at the bottom of the dispenser pushes candies within the dispenser (Okuda et al., 2016; Sherman et al., 2018).

All seven Lpt proteins are essential for the transportation of LPS and the survival of most Gram-negative bacteria. In particular, LptA, C, D, and E of the Lpt complex are predominantly localized in the periplasm or the OM, potentially reducing the necessity for intracellular drug accumulation (Sherman et al., 2014). Therefore, targeting these Lpt proteins has garnered significant attention as an innovative antibacterial approach. Antibacterial drug discovery strategies aimed at inhibiting the Lpt machinery have primarily focused on the following proteins: the ATPase LptB (Novobiocin analogs, Compound 1a) (May et al., 2017; Sherman et al., 2013), the OM pore LptD (POL7080) (Martín-Loeches et al., 2018; Shankaramma et al., 2003), the periplasmic protein LptA (Thanatin, IMB-881) (Ma et al., 2019; Moura et al., 2020; Vetterli et al., 2018; Zhang et al., 2019) and the TM protein LptF (Zosurabalpin) (Pahil et al., 2024; Zampaloni et al., 2024). In particular, POL7080 (murepavadin) progressed the furthest down the development pipeline but was withdrawn from phase III clinical trials due to concerns about toxicity (Sabnis & Edwards, 2023). Zosurabalpin is currently undergoing clinical development as a new antibiotic for combating *Acinetobacter* spp., including carbapenem-resistant *Acinetobacter baumannii* (CRAB) (Pahil et al., 2024; Zampaloni et al., 2024).

In this review, we aim to present a comprehensive summary of current research on the structural interactions within the Lpt complex and the function and regulation of LPS transport via the Lpt system. Additionally, we discuss the current efforts aimed at developing new antibiotics against the Lpt complex.

### Extraction of Mature LPS from the IM to the Periplasm: The LptB2FG-LptC Complex

The transfer of mature LPSs from the IM to the OM can be conceptually divided into the following stages, each involving distinct Lpt components: LPS extraction from

the IM, LPS translocation across the periplasm, and LPS export across the OM. The initial step in extracting LPS from the IM is carried out by the LptB2FG protein complex. LptB2FG is an IM ABC transporter that contains a cytoplasmic homodimeric nucleotide-binding domain (NBD), LptB, and the heterodimeric transmembrane domain (TMD) subunit, LptFG. Both LptF and LptG feature six TM helices (TM1–TM6), a substantial periplasmic domain adopting a  $\beta$ -jellyroll architecture, and a coupling helix that interacts with one LptB monomer on the cytoplasmic side (Dong et al., 2017; Ruiz et al., 2008; Sherman et al., 2014; Wang et al., 2014) (Fig. 2). The LptB protomer comprises a RecA-like domain and a helical domain, similar to other typical ATPases. The dimerization of LptB, facilitated by the presence of two ATP molecules is crucial for the extraction of LPS (Bertani et al., 2018; Sherman et al., 2014). Unlike most other ABC transporters that translocate substrates across the membrane, LptB2FG extracts LPS directly from the same leaflet of the membrane rather than switching it from one side of the membrane to another (Dong et al., 2017). Within the LptB2FG transporter, the LptF–LptG subunits create a central cavity that exhibits hydrophobic properties in the IM and is highly charged within the periplasm. Mutagenesis studies that target the hydrophobic and positively charged residues within this cavity, along with functional assays, have provided compelling evidence that the cavity may function as a binding site for LPS (Dong et al., 2017; Luo et al., 2017). Crucial structural insights were attained through cryo-electron microscopy (cryo-EM) analysis of the *Escherichia coli* LptB2FG complex in the presence of LPS (Li et al., 2019) (Fig. 2A). The results clearly show that the six lipid acyl chains of LPS snugly fit into a cone-shaped hydrophobic pocket formed by the TM1, TM2, and TM5 helices of both LptF (Leu307, Phe26) and LptG (Phe317, Phe367, and Tyr320). A ring of positively charged residues located at the periplasmic entrance of the pocket, which includes Lys34, Lys40, Lys41, Lys62, Arg133, and Arg136 of LptG, as well as Arg33, Lys30, and Lys317 of LptF, forms electrostatic interactions with the negatively charged phosphate groups of the bound LPS (Li et al., 2019). Indeed, mutagenesis studies have shown that replacing Arg33 with Glu in LptF resulted in cellular mortality, and altering the charge of Lys34, Lys40, and Lys41 in LptG caused defects in both LPS transport and bacterial growth (Bertani et al., 2018; Li et al., 2019). Interestingly, the complete LptB2FG complex represents substantially higher ATPase activity, but LptC inhibited the ATPase activity of LptB2FG in a proteoliposome system as well as nanodiscs (Li et al., 2019; Sherman et al., 2018). In the structures of LptB2FG and LptB2FGC from *Shigella flexneri*, the ATPase activity of LptB2FGC was approximately 50% lower than that of LptB2FG under the same conditions, confirming the regulatory role of LptC in the LptB2FG transporter (Tang et al., 2019).



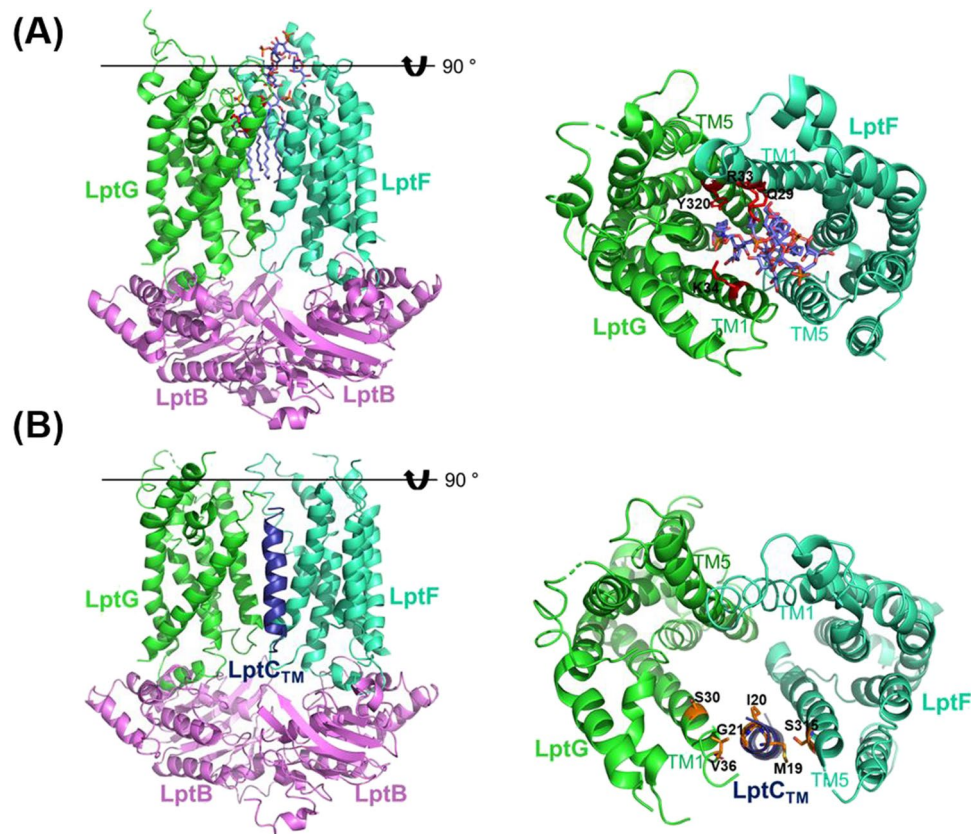


**Fig. 2** Cryo-EM structure of LptB2FGC in the absence or presence of LPS. **(A)** In the presence of LPS, as depicted in the cryo-EM structure (PDB: 6MUH), LptF, LptG, and two LptB subunits are colored green-cyan, green, and violet, respectively. The LPS, depicted in slate, is positioned between LptF and LptG. The newly synthesized LPS, situated in the IM, binds at the entry point delineated by the LptC TM helix, which intercalates between LptG TM1 and LptF TM5. In the top view of LptFG-bound LPS (for clarity, the LptB dimer is omitted), a ring of positively charged residues (Arg33 of LptF, Lys34 of LptG) at the periplasmic opening

of the pocket forms electrostatic interactions with the bound LPS. Additionally, Gln29 of LptF and Tyr320 of LptG engage in close contact with the acyl chains of the bound LPS. **(B)** The cryo-EM structure of nucleotide-free LptB2FGC from *E. coli* (PDB: 6MI7) reveals the interdigitation of the TM helix of LptC between LptF TM5 and LptG TM1. A top-down view of the periplasm illustrates the LPS-binding cavity formed by LptFGC in the depicted structure panel (for clarity, the LptB dimer is omitted). The interacting residues at TM1 of LptG, TM5 of LptF, and the TM helix of LptC are represented as sticks

Simson et al. postulated that LptFG directly extracts LPS via its LPS-binding domain or indirectly facilitates its transfer by inducing a conformational shift in LptC (Simpson et al., 2016). While the loss of the TM helix of LptC does not induce defects in bacterial growth or LPS transport on its own, a recent study has proposed two distinct physiological roles for the TM helix of LptC. First, it is essential for maintaining optimal levels of LptC. Second, it plays a role in coordinating the ATPase activity of LptB with LptFG before loading LPS onto the periplasmic bridge (Wilson & Ruiz, 2022). However, a detailed understanding of the mechanism is crucial to determine whether LptC's TM helix prevents premature closure of the LPS-binding cavity, ensuring proper binding of LPS and ATP, or coordinates with the placement of LPS onto the  $\beta$ -jellyroll of LptF.

Three structural studies have provided insights into LptB2FGC structures across various Gram-negative bacterial

strains. Owens et al. (2019) conducted an X-ray crystallographic analysis of *Vibrio cholerae* and *Enterobacter cloacae* LptB2FGC within detergent micelles. In another study, Li et al. (2019) utilized cryo-EM to examine *E. coli* LptB2FGC within lipid nanodiscs, both with and without ADP-vanadate. Tang et al. (2019) employed cryo-EM to investigate *S. flexneri* LptB2FGC in the presence of LPS or the ATP analog  $\beta$ - $\gamma$ -imidoadenosine 5'-triphosphate (AMP-PNP). According to these distinct cryo-EM studies of LptB2FGC, the periplasmic domain of LptC did not exhibit a well-defined density, possibly due to its flexibility. However, observations in both studies consistently revealed that the TM of LptC is located at a lateral gate between the TM1 of LptG and the TM5 of LptF (Li et al., 2019; Tang et al., 2019) (Fig. 2B). Gly21 from the TM of LptC interacts with Val36 of TM1 of LptG. On the other hand, the TM of LptC established a multitude of extensive hydrophobic

interactions with the TM5 of LptF, involving a sequence of Leu, Val, and Ile residues in both helices. Owens et al. (2019) demonstrated that LPS entry into the cavity occurs through a distinct route between LptG TM1 and LptF TM5, which aligns precisely with the location of the TM of LptC. This pathway directly aligns with the concave surface of the continuous  $\beta$ -jellyroll formed through the interaction of LptF and LptC. Additionally, another potential entry point between LptG TM5 and LptF TM1 is impeded by the steric barrier created by the convex surface of the continuous LptF–LptC  $\beta$ -jellyroll (Owens et al., 2019). The researchers conducted *in vivo* photocrosslinking experiments and found no observable crosslinks to LPS at the alternative entry point between TM5 of LptG and TM1 of LptF. Instead, crosslinks were detected at the following distinct sites: one within the cavity, defined by LptC Gly21 and LptG Ser30, and another at the interface between the LptF–LptC  $\beta$ -jellyroll complex. Crosslinking inside the cavity was still observed in the absence of ATP; in contrast, crosslinking to LptC Phe78 in the  $\beta$ -jellyroll was not detected under the same conditions (Owens et al., 2019). In the LptB2FGC structures of the Liao group in the presence of ADP-vanadate (Li et al., 2019), the cavity between TM1 of LptG and TM5 of LptF shows no observable LPS, which resulting from the strong dimerization of LptB. TM density of LptC is also not detected, however, showed a long  $\beta$ -jellyroll domain region, which indicates stably attached  $\beta$ -jellyroll of LptC to  $\beta$ -jellyroll of LptF. Thus, upon ATP binding, TM of LptC moves away from the TM1 of LptG–TM5 of LptF interface and becomes disordered, which facilitates  $\beta$ -jellyroll complex of LptF–LptC and allows the TMDs to rearrange. The sLptB2FGC structure bound to AMP-PNP demonstrated strong dimerization of LptB, leading to conformational shifts in the TMDs of LptFG. The residues Arg292 of LptF and Arg301 of LptG, identified as interacting with the bound nucleotides, may play a role in modulating the states of the lateral gates of LptB2FGC. This is because these residues are situated on loop2, which connects the respective TM5 of LptF and LptG, constituting the lateral gates. This results in a closed central cavity with an expansive opening at the periplasmic side of the cavity, potentially representing a postexport state of LPS (Owens et al., 2019).

Based on the reported structural and functional studies, the following model for LPS movement through LptB2FGC onto the LptA bridge is suggested. 1) LPS laterally enters the inner cavity between LptG TM1 and LptF TM5, where the TM of LptC is located, independent of ATP. 2) Due to LPS binding, the TM of LptC dissociates from the TMD interface between LptG and LptF, and the  $\beta$ -jellyroll of LptC stably associates with that of LptF. 3) Following the dimerization of LptB triggered by ATP binding, the constriction of the cavity, driven by ATP, generates the force necessary to expel LPS from the membrane. 4) More LPS molecules

are extracted by additional cycles of steps 1–3 and pushed toward the  $\beta$ -jellyroll of LptC. The TM of LptC coordinates ATP hydrolysis with LPS extraction from the IM, and the  $\beta$ -jellyroll of LptC binds to the  $\beta$ -jellyroll of LptF in the periplasm. Moreover, the gate within the  $\beta$ -jellyroll of LptF enhances transport efficiency by impeding the reverse movement of LPS back into the membrane when the cavity reopens. This mechanism ensures that LPSs flow in one direction from LptC to LptA and ultimately LptDE to reach the OM.

### The Periplasmic Lpt Bridge: LptA

The subsequent step in LPS transport to the OM involves the transfer of synthesized LPS through a periplasmic bridge formed by the protein LptA. This bridge links to the LptB2FGC complex via LptC, facilitating its span across the IM (Freinkman et al., 2012). LptC interacts with LptF through its  $\beta$ -jellyroll structure at the amino-terminal edge. Simultaneously, the carboxy terminus of LptC binds to the N-terminus of LptA. This interaction was confirmed by the copurification of the LptA–LptC complex observed during size-exclusion chromatography experiments (Bowyer et al., 2011; Freinkman et al., 2012; Sperandio et al., 2011). The translocation of LPS from LptB2FGC to LptA through LptC represents an additional distinct ATP-dependent stage of LPS transport (Okuda et al., 2012).

The crystal structure of LptA has been elucidated, revealing that LptA shares the same  $\beta$ -jellyroll fold as LptC, LptF, and LptG. This identical fold was also found in the periplasmic N-terminal domain of LptD. This observation suggested that small structurally homologous domains must adopt a common basic module, often referred to as the "Lpt fold," for periplasmic protein bridges to form (Botos et al., 2016; Qiao et al., 2014; Suits et al., 2008; Tran et al., 2010) (Fig. 3A). Inspection of the  $\beta$ -jellyroll structure of LptC revealed that could form a possible pocket for LPS binding, and this cavity contained hydrophobic residues oriented toward the interior structure (Tran et al., 2010). Additionally, the configuration of the  $\beta$ -jellyroll domains in LptC, LptA, and the N-terminal periplasmic segment of LptD creates an uninterrupted hydrophobic groove. This groove may provide space for the acyl chains of the lipid A moiety during LPS transport across the protein bridge, while the hydrophilic oligosaccharide portion remains exposed in the periplasm. LptA and LptC both bind LPS; therefore, the Lpt fold plays a crucial role in the transport of LPS (Okuda et al., 2012; Schultz et al., 2017; Sestito et al., 2014; Tran et al., 2010). LptA was initially considered to act as a soluble chaperone protein, similar to the periplasmic chaperone LolA, to shield the acyl chains of LPS during transport. However, in spheroplasts, newly synthesized LPS is observed to be transported to the OM, indicating that LPS transport might occur

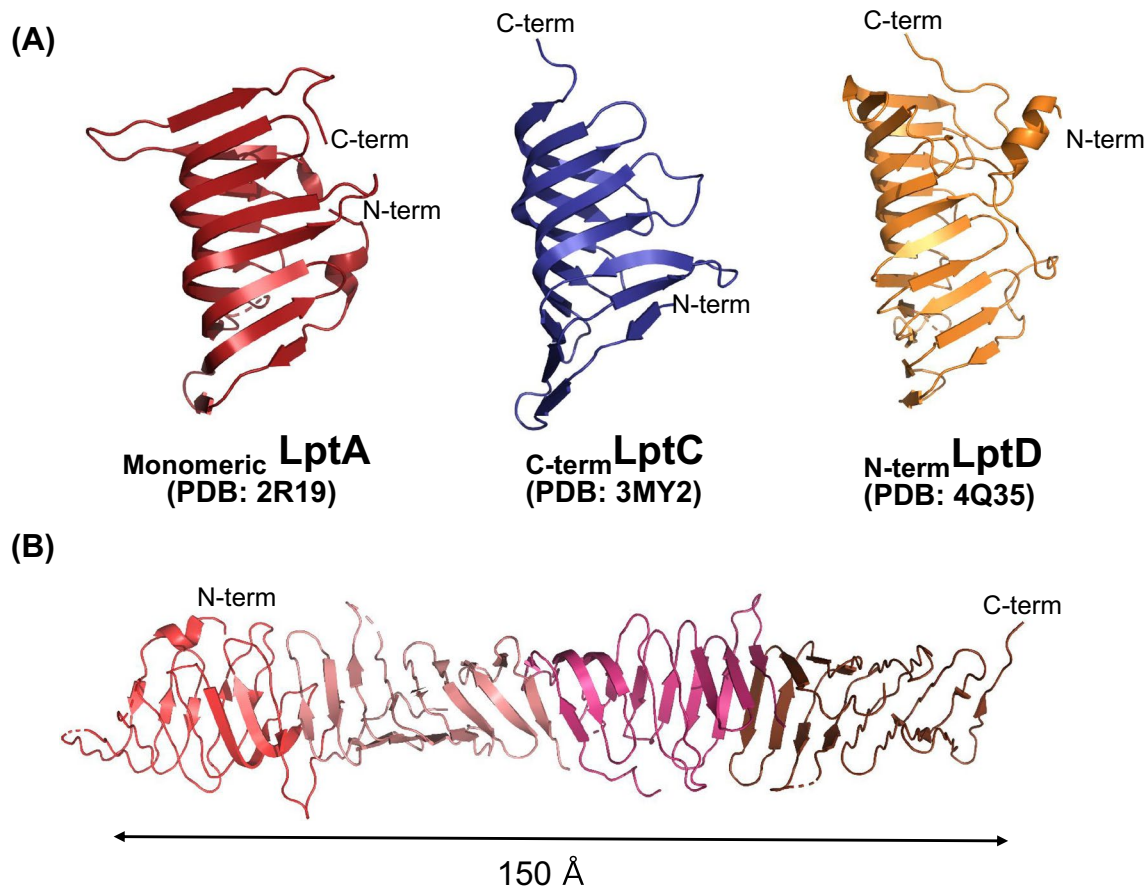


**Fig. 3** β-jellyroll fold (Lpt fold) of Lpt proteins. **(A)** Crystal structures of an LptA monomer (PDB: 2R19), LptC (PDB: 3MY2), and the N-terminal jellyroll domain in LptD (PDB: 4Q35) are depicted. An identical β-jellyroll fold is observed in LptA, LptC, and LptD, facilitating their interconnection to align their slots in an elongated

hydrophobic groove that winds across the space between the inner membrane (IM) and the outer membrane (OM). **(B)** The crystal structure of the LptA tetramer is presented, with subunits interacting in a head-to-tail manner (PDB: 2R1A)

through membrane contact sites. This phenomenon is supported by pulse-chase experiments, which demonstrated that LPS transport to the OM continues even after the soluble periplasmic components are removed (Tefsen et al., 2005). Biochemical investigations employing epitope-tagged LptB, LptC, and LptF have provided evidence that the LptA structure copurifies with LptD and LptE. This finding supports the concept that these proteins collectively form a continuous protein bridge that connects the IM and OM. (Chng et al., 2010a, 2010b). Mutations that impair LptC or deplete LptE and LptD result in the degradation of the periplasmic LptA component (Sperandeo et al., 2011). Taken together, these results indicate that a physical bridge of LptC-A-D forms, which serves as a conduit for LPS transport across the periplasmic space and effectively links the IM and OM.

Based on its single-crystal structure in the presence of LPS, LptA exists as a tetramer with monomeric subunits arranged end-to-end (Suits et al., 2008) (Fig. 3B). Each LptA monomer exhibits a 90° twist along its backbone, leading to

a helical hydrophobic groove in the periplasmic filament, which is formed by the aligned LptA proteins. The continuous hydrophobic groove could shield the lipid A portion of LPS molecules from the aqueous environment during LPS transport to the OM. Mass spectral analysis confirmed that LptA forms oligomers consisting of 2 to 5 members, and this oligomerization is concentration-dependent when LptA is purified in vitro and stabilized by LPS (Santambrogio et al., 2013). EPR spectroscopy experiments focusing on the interaction between LptC and LptA ( $K_d = 4 \mu\text{M}$ ) and LptA oligomerization ( $K_d = 29 \mu\text{M}$ ) revealed that the binding affinity between LptA and LptC surpasses the affinity observed for LptA oligomerization (Schultz et al., 2013). Nevertheless, the exact stoichiometry of LptA within the periplasmic protein bridge remains unclear. A truncated form of LptA (LptAm), created by eliminating the C-terminal β-sheet (Δ160–185) that could disrupt the LptA–LptA interaction, can still interact with LptC and transport LPS to the OM with partial functionality (Laguri et al., 2017). A single



LptA complex can bridge the intermembrane distance of 10 nm in *E. coli*. However, the OM can display a multitude of compositions, spatial heterogeneities, and rheological properties that influence its surrounding environment (Sun et al., 2021). Additionally, the width of the periplasmic space may vary among bacterial species and can be influenced by factors such as changes in osmotic conditions, thus resulting in considerable variability in the specific stoichiometry of LptA. In 2024, a comprehensive investigation combining gene deletion mutant analysis with deep-learning protein folding utilizing AlphaFold2 resulted in the prediction of the periplasmic bridge model comprising the LptCAD complex. According to this model, the assembly of a head-to-tail LptCAD complex is adequate to create a bridge that extends approximately 15 nm across the periplasmic space in *E. coli*. Additionally, the study confirmed that LptA can transiently oligomerize in the periplasm, thereby aiding in the formation of an extended bridge (Borrego & Burgas, 2024). Several studies have indicated that LptA possesses an additional  $\sigma^E$ -dependent promoter that becomes active under highly specific conditions, affecting LPS composition and biogenesis (Martorana et al., 2011; Sperandio et al., 2007). Enterobacteria can adapt to changes in periplasm width by employing RcsF, a stress sensor lipoprotein, in the Rcs stress response system (Asmar et al., 2017; Zietek

et al., 2022). The dynamic self-assembly of LptA provides the Lpt machinery with essential flexibility to adapt to variations in periplasmic width, especially under diverse stress conditions.

### Insertion of LPS into the OM Outer Leaflet: The LptDE Complex and the LptM

The last step in delivering and assembling LPS at the OM surface is mediated by the OM translocon, which consists of the  $\beta$ -barrel protein LptD and the lipoprotein LptE. The LptDE complex is the largest monomeric  $\beta$ -barrel protein identified to date and the only OM protein that adopts a barrel-and-plug architecture composed of two separate polypeptides (Chng et al., 2010b; Freinkman et al., 2011) (Fig. 4A). To date, the structural details of LptDE complexes have been elucidated for six pathogenic species, *S. enterica* (SeLptDE), *S. flexneri* (SfLptDE), *Yersinia pestis* (YpLptDE), *P. aeruginosa* (PaLptDE), *K. pneumoniae* (KpLptDE) and most recently, *Neisseria gonorrhoeae* (NgLptDE) (Botos et al., 2016; Botte et al., 2022; Dong et al., 2014; Qiao et al., 2014). Although the primary sequences exhibit divergences, such as a decrease of 25% between PaLptDE and SfLptDE, these structures demonstrated remarkable similarity. Structural conservation is also notable considering the wide range of

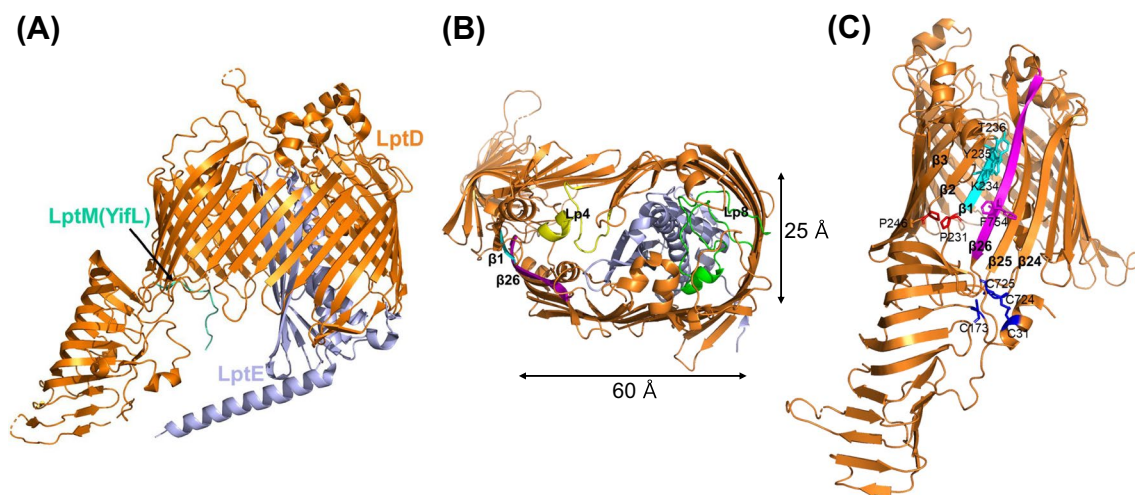


**Fig. 4** Structure of the plug-and-barrel complex of LptD, LptE, and LptM (YifL) located in the OM. (A) LptD is represented in orange, while LptE, which is embedded within the lumen of LptD, is illustrated in light blue. LptM (YifL) is colored green-cyan (PDB: 8H1R). During transport, the lipid A moiety of LPS binds to the N-terminal domain of LptD and is directly inserted into the membrane through a luminal gate positioned between the core domain and the N-terminal domain of LptD. Extracellular view of the LptD (orange)-LptE (light blue) complex. Lp4 (yellow) and Lp8 (green) are located in the interior of the barrel and other loops at the surface of the barrel pore. (B) The extracellular perspective of the LptD (orange)-LptE (light blue) complex reveals the presence of

Lp4 (yellow) and Lp8 (green) within the interior of the barrel, along with other loops on the surface of the barrel pore. (C) A lateral view of LptD (orange) is presented (LptE is omitted for clarity). The saccharide portion of LPS traverses through the luminal gate created by  $\beta$ -strands 1 and 26 of the C-terminal domain of LptD. The barrel may open during LPS insertion between  $\beta$ -strands 1 and 26, highlighted in cyan and magenta, respectively (PDB: 4Q35). Disulfide bonds formed by four cysteines, highlighted in blue, connect the N-terminal domain of LptD to its C-terminal domain. Proline residues on  $\beta$ 1 and  $\beta$ 26 (P231 and P246) restrict the ability of the strand to form a sheet, allowing  $\beta$ 1 and  $\beta$ 2 to separate. Additionally, the residues that interact between  $\beta$ 1 and  $\beta$ 26 are indicated

LPS substrates and the dramatic O-antigen variability among Gram-negative species. The N-terminal domain of LptD is a  $\beta$ -jellyroll that extends from the periplasm and forms a hydrophobic groove, providing continuity with the groove of LptA when LptD and LptA associate in vivo (Grabowicz et al., 2013; Sperandio et al., 2011; Suits et al., 2008; Villa et al., 2013). According to the structure of the SfLptDE complex, the C-terminal transmembrane portion forms a substantial 26-strand  $\beta$ -barrel ( $\beta$ 1– $\beta$ 26) that measures approximately  $65 \text{ \AA} \times 35 \text{ \AA}$  in the periplasmic direction and  $60 \text{ \AA} \times 25 \text{ \AA}$  in the extracellular direction (Fig. 4B). Given that LPS typically comprises six fatty acyl chains, each measuring  $25 \text{ \AA}$  in length and  $5 \text{ \AA}$  in width, this structure is sufficient to facilitate the crossing of LPS through the OM bilayer (Dong et al., 2014). This finding suggests that the  $\beta$ -jellyroll directly inserts lipid A into the membrane through a two-portal mechanism, while the oligosaccharide component advances through the hydrophilic lumen of the  $\beta$ -barrel. When examining the interface between the N-terminal domain and the C-terminal barrel domain of LptD, two distinct points of contact became evident (Fig. 4C). First, disulfide bonds formed by four cysteines connect the N-terminal domain to the  $\beta$ -barrel, specifically between  $\beta$ 24 and  $\beta$ 25. Structural and functional data indicate that the correct folding of LptD proteins involves several steps of disulfide bond reorganization, with at least one disulfide bond (Ruiz et al., 2010). Second, the N-terminal domain also connects to the  $\beta$ -barrel through a flexible linker polypeptide (luminal loop 1). Then, the start of  $\beta$ 1 is anchored by conserved proline residues, such as P230 in KpLptD, P231 in SfLptD, and P261 in NgLptD. With another conserved proline residue situated in the middle of the  $\beta$ 2 strand, the residues seem to disrupt the secondary structure of the strands, thereby preventing the typical  $\beta$ -sheet hydrogen bond from forming between the  $\beta$ 1 and  $\beta$ 26 strands (Fig. 4C). This creates a local gap, serving as a gateway for the lateral migration of LPS molecules between the LptDE complex and the membrane. When mutations were introduced at these two proline residues, the P231A/P246A double mutant of EcLptDE exhibited a severe phenotype, suggesting that the complex becomes nonfunctional and the optimal lateral gate operation is hindered (Botos et al., 2016). Additionally, mutations that introduce disulfide bonds between  $\beta$ 1 and  $\beta$ 26 result in lethal phenotypes (Dong et al., 2014). Despite the insights gained from functional data and molecular dynamics (MD) simulations, direct evidence of a lateral opening in X-ray crystallographic structures of LptD has remained elusive. However, recent advances in cryo-EM have provided clarity on this matter. The cryo-EM structure of NgLptDE has revealed a laterally opened configuration, shedding light on LPS translocation (Botte et al., 2022). In this fully opened structure, the  $\beta$ -barrel of LptD extends without hydrogen bonds between  $\beta$ 1 and  $\beta$ 26. There is a separation of

approximately  $10 \text{ \AA}$  between the extracellular ends and  $15 \text{ \AA}$  between the periplasmic ends of these strands. This separation results in a significantly large, continuous, solvent-accessible channel extending from the extracellular space through the barrel to the periplasm, providing ample space for transiting LPS molecules. The NgLptDE structure also shows a wider diameter of the barrel lumen, reflecting a more open conformation of the luminal gate (Botte et al., 2022).

The LptE lipoprotein adopts a roll-like structure composed of two closely associated  $\alpha$ -helices (H1 and H2) and a 4-strand  $\beta$ -sheet (S1–S4) situated within the lumen of LptD (Botos et al., 2016; Dong et al., 2014; Qiao et al., 2014). In the LptDE complex, approximately 75% of LptE is located inside the  $\beta$ -barrel of LptD. LptE is located in the larger lobe of LptD, while the smaller lobe, positioned near the  $\beta$ 1/ $\beta$ 26 junction, remains predominantly open and measures approximately  $30 \text{ \AA}$  in diameter at the periplasmic opening, tapering toward the extracellular side (Botos et al., 2016; Malojčić et al., 2014). The  $\beta$ -strands within the LptD barrel are interconnected by 13 loops (Lp1–Lp13), which predominantly reside on the surface of the pore, except for Lp4 and Lp8. These two loops are positioned within the interior of the barrel and play a role in the interactions between LptD and LptE (Dong et al., 2014) (Fig. 4B). Instead of directly transporting LPS, LptE may perform the following functions in LPS transport: assisting in the assembly of functional LptD, maintaining membrane impermeability, and assisting in the insertion of LPS into the cell surface. The assembly of functional LptD relies on the assistance of the BAM ( $\beta$ -barrel assembly machinery) complex and the extensive reshuffling of disulfide bonds. LptD, which lacks the correct disulfide bond configuration, cannot bind LptA or facilitate LPS export. LptE helps promote the formation of mature LptD, which contains two disulfide bonds between nonconsecutive cysteines (Chimalakonda et al., 2011; Denoncin et al., 2010; Wu et al., 2005). Extracellular Lp4 and Lp8 from the LptD insert inside the barrel bind to the LptE protein, which plugs the pore, thus preserving membrane permeability. According to recent functional studies, the depletion of *lptE* markedly decreases the levels of functionally assembled *lptD*, which plays a critical role in bacterial virulence in *P. aeruginosa*. (Lo Sciuto et al., 2018).

LptE has been demonstrated to effectively bind and disassemble surface-bound aggregates of LPS in vitro (Chng et al., 2010b; Malojčić et al., 2014). Using surface plasmon resonance (SPR), researchers investigated the interaction between wild-type LptE and mutant LptE variants (R91D, K136D) with LPS. The results indicate that residues R91 and K136 form an LPS-binding site on LptE, aiding in the solubilization of LPS by altering its interactions with other LPS molecules. Additionally, LPS:LptE complexes were examined at a 4:1 ratio through transmission electron



microscopy (TEM) revealed that filamentous-like LPS aggregates disappeared in the presence of wild-type LptE; in contrast, LptE mutants (R91D, K136D) did not exhibit this effect. Consequently, it can be inferred that LptE disrupts strong LPS–LPS interactions, thereby influencing the propensity of LPS to aggregate (Malojčić et al., 2014).

In 2023, a recently discovered lipoprotein, LptM (formerly known as YifL), was reported in *Enterobacteriaceae* (Yang et al., 2023). This protein assembles alongside LptD and LptE at the BAM complex. During the purification of LptD and LptE proteins in the absence of LptM, the amount of oxidized LptD significantly decreased. Additionally, the inactivation of LptM necessitates disulfide bond isomerization by DsbC for cell viability. While further structural and functional investigations are imperative, it is conceivable that LptM plays a role in facilitating the oxidative maturation of LptD, thereby activating the LPS translocon (Yang et al., 2023).

### Overall Mechanism of LPS Transport

The overall mechanism of the Lpt system is often metaphorically likened to "PEZ" candy dispensers (Okuda et al., 2016) (Fig. 1). According to this model, Lpt proteins operate in a manner akin to PEZ candy dispensers, in which a spring at the dispenser's base propels the candies within the dispenser. In the Lpt system, LPS molecules (resembling candies) residing in the outer leaflet of the IM are pushed toward LptC through the action of LptB2FG, which acts as the spring. This process relies on ATP hydrolysis by LptB in the cytoplasm. Following this, LPS is propelled from LptC to LptA (acting as the chamber) and traverses the Lpt periplasmic bridge toward the LptDE translocon (resembling the cap). According to the proposed model, LPS then traverses the translocon, and the lipid portion of LPS is directly inserted into the outer leaflet of the OM without entering the lumen of the LptD barrel. Meanwhile, the sugar portion of the LPS travels through the barrel. However, the continuous protein bridge formation that underlies the PEZ model has not been validated in living cells. Additionally, this PEZ model fails to describe how individual Lpt subunits bind and release LPS.

In 2023, Törk et al. (2023) demonstrated a transient LPS transport bridge through single-molecule tracking dynamics. By tracking the motion of individual endogenous Lpt proteins fused with the Halo tag and employing cumulative distribution function (CDF) analysis, the researchers confirmed that the immobile state of LptA, LptB, and LptC reflects the formation of the Lpt bridge. When the lifetimes of the immobile states of these proteins were measured in the presence or absence of LPS, the depletion of LPS resulted in a lower rate of bridge formation, causing LptA in the bridged state to destabilize. Additionally, based on half-life studies

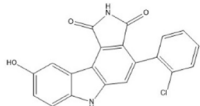
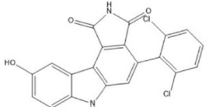
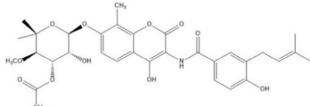
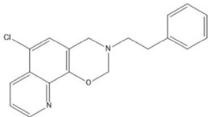
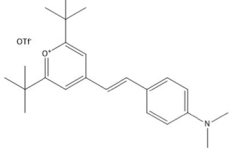
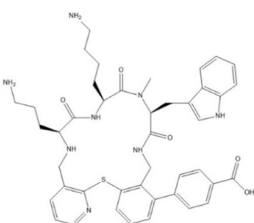
of the Lpt bridge with the LptC–LptA fusion protein, LptA preferentially associates with LptDE before forming a bridge with LptB2FGC. In summary, the authors proposed the following model for bridge formation and breakage (Törk et al., 2023): during bridge formation, the LPS-loaded LptB2FGC complex facilitates the formation of a bridge with LptA-bound LptDE, enabling the rapid transport of LPS to the OM. Conversely, for bridge breakage, the faster rate is associated with the absence of structural LPS (corresponding to two different bridge states), leading to breakage at the LptC–LptA interface. The slower rate is linked to the presence of structural LPS, stabilizing the LptC–LptA interface and causing breakage at the more stable LptD–LptA interface.

### Inhibitors Targeting LPS Transport

Due to the essentiality of its function, the Lpt protein complex has been studied as a target protein for new antibiotics (Table 1). The initial protein in the LPS transporter (LptB) hydrolyzes ATP to generate energy for pulling LPS from the IM to the OM. Due to this crucial role, LptB has become a focus in the development and screening of new antimicrobial agents effective against Gram-negative bacteria. One such screen was performed using 244 small molecule kinase inhibitors from two commercially available libraries; the best compound identified was 1a (a potent inhibitor of Weel), which blocks the ATPase activity of LptB (Gronenberg & Kahne, 2010). Unfortunately, the compound was only effective with a permeable OM, rendering it inactive against wild-type *E. coli* due to challenges in membrane penetration. Additionally, an enhanced iteration of Compound 1a (designated 1b) significantly impeded single LptB-mediated ATP hydrolysis. However, the inhibitory impact of Compound 1b diminished sixfold when tested against the LptB2FGC complex (Sherman et al., 2013). A cocrystal structure obtained also indicated that novobiocin, an antibiotic designed for bacterial DNA gyrase, binds to the LptB residue F90, which interacts with LptFG in *E. coli* (May et al., 2017). Interestingly, novobiocin not only stimulates the ATPase activity of this ABC transporter but also enhances polymyxin activity by promoting LPS transport (Mandler et al., 2018; May et al., 2017). However, the feasibility of novobiocin targeting the LptB2FGC transporter through direct chemical inhibition or synergistic effects via ATPase stimulation has not been fully explored.

In contrast to LptB inhibitors, which must traverse both bacterial membranes to reach their target, the most extensively studied component of the LPS transport machinery during the development of new drugs has been LptD, a surface-exposed protein. The first group of LptD inhibitors was unexpectedly discovered in a collection of peptidomimetic antibiotics. After the

**Table 1** Inhibitors targeting the LPS transporter

Target	Name	Structure	Origin & Screening method	Mechanism	Stage of development	References
LptB	Compound 1a		The compounds were selected among 244 small molecule kinase inhibitors and SAR research	They are ATP-competitive kinase inhibitors	They showed no activity in wild type <i>E. coli</i>	Gronenberg & Kanhe (2010); Sherman et al. (2013)
	Compound 1b					
	Novobiocin		The coumarin-derived compound was obtained from <i>Streptomyces niveus</i>	It binds to the LptB and stimulates ATPase activity	In preclinical discovery stage	May et al. (2017)
LptA	Thanatin	<i>P. maculiventris</i> : GSKKPVPPIIYCNRRTGKQCRM IUPAC Condensed: H-Gly-Ser-Lys-Lys-Pro-Val-Pro-Ile-Ile-Tyr-Cys(1)-Asn-Arg-Arg-Thr-Gly-Lys-Cys(1)-Gln-Arg-Met-OH	Thanatin was isolated from insects	Thanatin and its analogs inhibit both LptA-LptA and LptA-LptC interactions based on their high affinity for LptA (LptAm)	In preclinical discovery stage	Fehlbaum et al. (1996); Schuster et al. (2023); Sinha et al. (2022)
	IMB-881		The compound was selected by yeast two-hybrid assays with a library of 5,000–100,000 compounds	It blocks LptA/LptC interaction by specifically binding to LptA	The growth inhibition by the IMB compounds of gram-negative bacterial strains was demonstrated	Zhang et al. (2019)
	IMB-0042			It blocks LptA/LptC interaction by binding both LptA and LptC		Dai et al. (2022)
LptD	Murepavadin (POL7080)	IUPAC condensed: cyclo[Ala-Ser-D-Pro-Pro-Thr-Trp-Ile-Dab-Orn-D-Dab-Dab-Trp-Dab-Dab]	The compound was obtained from libraries of $\beta$ -hairpin-shaped peptidomimetics based on the protegrin I (PG-I) and SAR research	It interacts with <i>Pseudomonas</i> LptD	A phase 1b/2a trial of inhaled murepavadin is planned in adults with Cystic fibrosis	Robinson et al. (2005); Shankaramma et al. (2003); Srinivas et al. (2010); Li & Schneider-Futschik (2023)
LptFG	Zosurabalpin (RG6006)		The compound was obtained from whole-cell phenotypic screening of 44,985 MCPs from Tranzyme Pharma and SAR research	It traps LPS in <i>Acinetobacter</i> LptB <sub>2</sub> FGC complex binding with the TM helices of LptF and LptG and competing with the LptC TM helix	Currently in Phase I for <i>Acinetobacter</i> Infections under clinical development by F. Hoffmann-La Roche	Zampaloni et al. (2024); Pahil et al. (2024)

library was screened, which included  $\beta$ -hairpin peptidomimetic compounds based on the chemical structure of the antimicrobial peptide protegrin-1 by Polyphor (now incorporated as Spexis), multiple hits were revealed that specifically targeted LptD and affected bacterial growth (Robinson et al., 2005; Shankaramma et al., 2003). After extensive lead optimization, which

included considerations for stability in plasma, reduced hemolysis, and enhanced potency against *P. aeruginosa*, murepavadin (POL7080) was ultimately identified as the first-in-class novel antipseudomonal antibiotic (Martín-Loeches et al., 2018; Srinivas et al., 2010). Murepavadin directly binds to the N-terminal domain of LptD, a feature that distinguishes it from LptD in other

Gram-negative bacteria. This specific binding leads to the obstruction of LPS movement (Andolina et al., 2018; Sader et al., 2018; Schmidt et al., 2013). Preclinical testing of murepavadin yielded highly successful results, as the inhibitor exhibited bactericidal activity against more than 1200 clinical strains of *P. aeruginosa*. (Díez-Aguilar et al., 2020; Sader et al., 2018). In various murine infection models, murepavadin has shown outstanding in vivo efficacy, penetrating epithelial lung fluid effectively (Amponnawarat et al., 2021; Melchers et al., 2019; Wach et al., 2018). These encouraging results led to the advancement of murepavadin into phase II clinical trials, during which it exhibited efficacy in the treatment of ventilator-associated pneumonia caused by *P. aeruginosa* (MacNair et al., 2020; Upert et al., 2021). During Phases I and II, murepavadin was tested as a monotherapy. However, due to ethical considerations in phase III trials involving pneumonia patients, murepavadin was coadministered with ertapenem, a broad-spectrum  $\beta$ -lactam antibiotic. Consequently, the advancement of phase III studies for murepavadin was temporarily paused in May 2019 due to a higher incidence of acute kidney injury (56% in the treatment group compared to 20% in the control group) (Prasad et al., 2022). However, murepavadin was the only clinically active Gram-negative bacterial candidate in this decade that was discontinued after Phase III. Spexis continued the preclinical development of an inhalation formulation of murepavadin, and clinical phase I trial authorization was granted in the United Kingdom in December 2020 (Li & Schneider-Futschik, 2023).

Thanatin, a 21-amino acid peptide derived from the hemipteran insect *Podisus maculiventris*, was initially characterized in 1996 and has demonstrated broad-spectrum antibacterial activity (Fehlbaum et al., 1996). Recent work by the Robinson group revealed that the effectiveness of thanatin against Gram-negative bacteria primarily results from its interaction with LptA and LptD. This conclusion was supported by a range of experiments, including biochemical, biophysical, structural biology, and genetic analyses (Fiorentino et al., 2021b; Vetterli et al., 2018). By utilizing a bacterial adenylate cyclase two-hybrid system, thanatin disrupted the interactions between LptA–LptA and LptA–LptC, consequently inhibiting LPS transport across the periplasm (Moura et al., 2020). Through systematic and structure-based SAR exploration, optimized analogs of thanatin, namely, Compounds 6 and 7, were found to exhibit potent in vitro and in vivo antimicrobial activity in mouse models. These compounds demonstrated favorable absorption, distribution, metabolism, and excretion (ADME) characteristics,

along with low nanomolar binding affinity to both LptA and the thanatin-resistant LptA Q62L mutant (Schuster et al., 2023). An analog, thanatin M21F, also showed superior antibacterial activity and displayed increased binding affinity ( $K_d \sim 0.73$  nM) for LptA compared to that observed for thanatin (13 nM  $K_d$ ) (Sinha et al., 2022).

Two small molecules, IMB-881 and IMB-0042, were recently identified through a yeast two-hybrid screen designed to detect the inhibition of the LptA–LptC interaction (Dai et al., 2022; Zhang et al., 2019). These molecules were selected based on their demonstrated antimicrobial activity against Enterobacterial species. Furthermore, the inhibitory effect of IMB-881 on protein–protein interactions within the Lpt complex, including interactions with the *P. aeruginosa* LptA homolog LptH, was investigated using a native mass spectrometry-based approach (Bollati et al., 2015; Fiorentino et al., 2021a). Nevertheless, additional studies are needed to provide clear evidence of the effectiveness of these compounds.

Very recently (in January 2024), two remarkable articles were published in Nature, one by industry (Roche) and the other by academia (Harvard University), that discussed zosurabalpin, an antibacterial macrocyclic peptide (MCP) that targets LptF to trap LPS (Pahil et al., 2024; Zampaloni et al., 2024). In the first paper, Zampaloni et al. at Roche identified RO7036668, which selectively kills *A. baumannii*, through whole-cell phenotypic screening of 44,985 MCPs. This compound was further optimized for efficacy and tolerability, resulting in the selection of the zwitterionic benzoic acid derivative zosurabalpin, which exhibited improved solubility and safety characteristics. To identify the compound's potential molecular target, the authors generated resistance to increasing concentrations of zosurabalpin using a morbiostat system. They observed common mutations in E249, I317, R322, and I323 of LptF across multiple *A. baumannii* strains, suggesting that the compounds could interfere with LPS transport, leading to cell death from the abnormal accumulation of toxic LPS inside the cell. In the second paper, Pahil and colleagues solved the cryo-EM structure of the zosurabalpin–LptB2FG complex at a resolution of 3.6 Å. The binding pocket of the compound is formed by the side chains of several amino acids in the TM helices of LptF (E58, E249, W271, V314, I317, R320, and T321) and LptG (L36). Additionally, in vitro ATPase activity assays and a scintillation proximity assay (SPA) revealed that zosurabalpin interacts with LptB2FGC only when the complex is bound to LPS, causing the LptC TM helix to dissociate from the complex. Hence, the presence of LPS is indispensable for the drug's mode of action. Zosurabalpin shows



promising potential for clinical use due to its potent antibacterial efficacy against carbapenem-resistant *A. baumannii* (CRAB) and pandrug-resistant *Acinetobacter* strains. The drug has been evaluated in two phase I clinical trials as a new class of antibiotic that targets *Acinetobacter* infections (Guenther et al., 2023).

## Conclusion

Focusing on LPS biosynthesis and transport machinery is an appealing therapeutic approach, as the LPS provides an essential barrier function in most Gram-negative bacteria. This approach holds promise for developing potential broad-spectrum agents with efficacy against multiple Gram-negative bacteria. However, despite the allure of targeting LPS transport, significant barriers currently impede the development of corresponding inhibitors for patient use. First, there is a potential for frequent drug resistance. To date, most LPS-directed inhibitors, including Lpt-targeted inhibitors, are single-target agents, raising concerns about their potential for the development of target-based resistance (Silver, 2011; Theuretzbacher et al., 2023; Zhang et al., 2018). Second, LPS is not essential in certain *Moraxella* species, such as *Neisseria meningitidis*, *Moraxella catarrhalis*, and *A. baumannii*, which could be a challenge (Moffatt et al., 2010; Peng et al., 2005; Steeghs et al., 2001; Zhang et al., 2013). In addition, zosurabalpin may not be effective against LPS-deficient *A. baumannii*, although its therapeutic potential is promising for the treatment of most *Acinetobacter* infections. Finally, there are issues involving host toxicity and poor solubility, particularly with small molecule inhibitors with hydrophobic groups that impact solubility and increase serum protein binding.

Recent strides in understanding LPS transport have been notable, especially advancements in key structural insights during this process. Despite the absence of clinically approved antibiotics targeting LPS transport, significant research endeavors have focused on discovering and refining these antibiotics, employing a wide range of discovery strategies. In essence, owing to their indispensable role, difference in mammalian hosts and beneficial taxa, and presence in hypervirulent strains, Lpt proteins continue to emerge as promising targets for the development of antimicrobial drugs effective against various opportunistic pathogens. Thus, inhibitors aimed at the LPS transport system represent a potential frontier in the realm of first-in-class antibiotics.

**Acknowledgements** This work received support from the Korea Research Institute of Chemical Technology (KK2432-10). We extend our sincere gratitude to Dr. Jae Woo Park from Chungbuk National University and Dr. Hyuk Lee from KRICT for their invaluable comments and assistance in completing this research.

## Declarations

**Conflict of Interest** The author declares no competing financial interest.

## References

- Amponnawarat, A., Ayudhya, C. C. N., & Ali, H. (2021). Murepavadin, a small molecule host defense peptide mimetic, activates mast cells via MRGPRX2 and MRGPRB2. *Frontiers in Immunology*, 12, 689410.
- Andolina, G., Bencze, L. C., Zerbe, K., Müller, M., Steinmann, J., Kocherla, H., Mondal, M., Sobek, J., Moehle, K., Malojčić, G., et al. (2018). A peptidomimetic antibiotic interacts with the periplasmic domain of LptD from *Pseudomonas aeruginosa*. *ACS Chemical Biology*, 13, 666–675.
- Ashraf, K. U., Nygaard, R., Vickery, O. N., Erramilli, S. K., Herrera, C. M., McConville, T. H., Petrou, V. I., Giacometti, S. I., Dufrisque, M. B., Nosol, K., et al. (2022). Structural basis of lipopolysaccharide maturation by the O-antigen ligase. *Nature*, 604, 371–376.
- Asmar, A. T., Ferreira, J. L., Cohen, E. J., Cho, S., Beeby, M., Hughes, K. T., & Collet, J. F. (2017). Communication across the bacterial cell envelope depends on the size of the periplasm. *PLoS Biology*, 15, e2004303.
- Bertani, B. R., Taylor, R. J., Nagy, E., Kahne, D., & Ruiz, N. (2018). A cluster of residues in the lipopolysaccharide exporter that selects substrate variants for transport to the outer membrane. *Molecular Microbiology*, 109, 541–554.
- Bollati, M., Villa, R., Gourlay, L. J., Benedet, M., Dehò, G., Polissi, A., Barbiroli, A., Martorana, A. M., Sperandeo, P., Bolognesi, M., et al. (2015). Crystal structure of LptH, the periplasmic component of the lipopolysaccharide transport machinery from *Pseudomonas aeruginosa*. *The FEBS Journal*, 282, 1980–1997.
- Borrego, J. G., & Burgas, M. T. (2024). Structural assembly of the bacterial essential interactome. *eLife*, 13, e94919.
- Bos, M. P., Tefsen, B., Geurtsen, J., & Tommassen, J. (2004). Identification of an outer membrane protein required for the transport of lipopolysaccharide to the bacterial cell surface. *Proceedings of the National Academy of Sciences of the United States of America*, 101, 9417–9422.
- Botos, I., Majdalani, N., Mayclin, S. J., McCarthy, J. G., Lundquist, K., Wojtowicz, D., Barnard, T. J., Gumbart, J. C., & Buchanan, S. K. (2016). Structural and functional characterization of the LPS transporter LptDE from Gram-negative pathogens. *Structure*, 24, 965–976.
- Botte, M., Ni, D., Schenck, S., Zimmermann, I., Chami, M., Bocquet, N., Egloff, P., Bucher, D., Trabuco, M., Cheng, R. K. Y., et al. (2022). Cryo-EM structures of a LptDE transporter in complex with Pro-macrobodies offer insight into lipopolysaccharide translocation. *Nature Communications*, 13, 1826.
- Bowyer, A., Baardsnes, J., Ajamian, E., Zhang, L., & Cygler, M. (2011). Characterization of interactions between LPS transport proteins of the Lpt system. *Biochemical and Biophysical Research Communications*, 404, 1093–1098.

- Caroff, M., & Novikov, A. (2020). Lipopolysaccharides: Structure, function and bacterial identifications. *Oilseeds and Fats, Crops and Lipids*, 27, 31.
- Chimalakonda, G., Ruiz, N., Chng, S., Garner, R. A., Kahne, D., & Silhavy, T. J. (2011). Lipoprotein LptE is required for the assembly of LptD by the  $\beta$ -barrel assembly machine in the outer membrane of *Escherichia coli*. *Proceedings of the National Academy of Sciences of the United States of America*, 108, 2492–2497.
- Chng, S., Gronenberg, L. S., & Kahne, D. (2010a). Proteins required for lipopolysaccharide assembly in *Escherichia coli* form a transenvelope complex. *Biochemistry*, 49, 4565–4567.
- Chng, S., Ruiz, N., Chimalakonda, G., Silhavy, T. J., & Kahne, D. (2010b). Characterization of the two-protein complex in *Escherichia coli* responsible for lipopolysaccharide assembly at the outer membrane. *Proceedings of the National Academy of Sciences of the United States of America*, 107, 5363–5368.
- Dai, X., Yuan, M., Lu, Y., Zhu, X., Liu, C., Zheng, Y., Si, S., Yuan, L., Zhang, J., & Li, Y. (2022). Identification of a small molecule that inhibits the interaction of LPS transporters LptA and LptC. *Antibiotics*, 11, 1385.
- Denoncin, K., Vertommen, D., Paek, E., & Collet, J. (2010). The Protein-disulfide isomerase DsbC cooperates with SurA and DsbA in the assembly of the essential  $\beta$ -barrel protein LptD. *Journal of Biological Chemistry*, 285, 29425–29433.
- Díez-Aguilar, M., Hernández-García, M., Morosini, M., Fluit, A., Tunney, M. M., Huertas, N., Del Campo, R., Obrecht, D., Bernardini, F., Ekkelenkamp, M., et al. (2020). Murepavadin antimicrobial activity against and resistance development in cystic fibrosis *Pseudomonas aeruginosa* isolates. *Journal of Antimicrobial Chemotherapy*, 76, 984–992.
- Doerrler, W. T., Gibbons, H. S., & Raetz, C. R. H. (2004). MsbA-dependent translocation of lipids across the inner membrane of *Escherichia coli*. *Journal of Biological Chemistry*, 279, 45102–45109.
- Dong, H., Xiang, Q., Gu, Y., Wang, Z., Paterson, N. G., Stansfeld, P. J., He, C., Zhang, Y., Wang, W., & Dong, C. (2014). Structural basis for outer membrane lipopolysaccharide insertion. *Nature*, 511, 52–56.
- Dong, H., Zhang, Z., Tang, X., Paterson, N. G., & Dong, C. (2017). Structural and functional insights into the lipopolysaccharide ABC transporter LptB<sub>2</sub>FG. *Nature Communications*, 8, 222.
- Fehlbaum, P., Bulet, P., Chernysh, S., Briand, J. P., Roussel, J. P., Letellier, L., Hetru, C., & Hoffmann, J. A. (1996). Structure-active analysis of thanatin, a 21-residue inducible insect defense peptide with sequence homology to frog skin antimicrobial peptides. *Proceedings of the National Academy of Sciences of the United States of America*, 93, 1221–1225.
- Fiorentino, F., Rotili, D., Mai, A., Bolla, J. R., & Robinson, C. V. (2021a). Mass spectrometry enables the discovery of inhibitors of an LPS transport assembly via disruption of protein–protein interactions. *Chemical Communications*, 57, 10747–10750.
- Fiorentino, F., Sauer, J. B., Qiu, X., Corey, R. A., Cassidy, C. K., Mynors-Wallis, B., Mehmood, S., Bolla, J. R., Stansfeld, P. J., & Robinson, C. V. (2021b). Dynamics of an LPS translocon induced by substrate and an antimicrobial peptide. *Nature Chemical Biology*, 17, 187–195.
- Freinkman, E., Chng, S., & Kahne, D. (2011). The complex that inserts lipopolysaccharide into the bacterial outer membrane forms a two-protein plug-and-barrel. *Proceedings of the National Academy of Sciences of the United States of America*, 108, 2486–2491.
- Freinkman, E., Okuda, S., Ruiz, N., & Kahne, D. (2012). Regulated assembly of the transenvelope protein complex required for lipopolysaccharide export. *Biochemistry*, 51, 4800–4806.
- Grabowicz, M., Yeh, J., & Silhavy, T. J. (2013). Dominant negative *lptE* mutation that supports a role for LptE as a plug in the LptD barrel. *Journal of Bacteriology*, 195, 1327–1334.
- Gronenberg, L. S., & Kahne, D. (2010). Development of an activity assay for discovery of inhibitors of lipopolysaccharide transport. *Journal of the American Chemical Society*, 132, 2518–2519.
- Gu, Y., Stansfeld, P. J., Zeng, Y., Dong, H., Wang, W., & Dong, C. (2015). Lipopolysaccharide is inserted into the outer membrane through an intramembrane hole, a lumen gate, and the lateral opening of LptD. *Structure*, 23, 496–504.
- Guenther, A., Millar, L., Messer, A., Giraudon, M., Patel, K., Deurloo, E. J., Lobritz, M., & Gloger, A. (2023). 2126. Safety, tolerability, and pharmacokinetics (PK) in healthy participants following single dose administration of zosurabalpin, a novel pathogen-specific antibiotic for the treatment of serious *Acinetobacter* infections. *Open Forum Infectious Diseases*, 10, ofad500.1749.
- Laguri, C., Sperandio, P., Pounot, K., Ayala, I., Silipo, A., Bougault, C. M., Molinaro, A., Polissi, A., & Simorre, J. (2017). Interaction of lipopolysaccharides at intermolecular sites of the periplasmic Lpt transport assembly. *Scientific Reports*, 7, 9715.
- Li, D., & Schneider-Futschik, E. K. (2023). Current and emerging inhaled antibiotics for chronic pulmonary *Pseudomonas aeruginosa* and *Staphylococcus aureus* infections in cystic fibrosis. *Antibiotics*, 12, 484.
- Li, X., Gu, Y., Dong, H., Wang, W., & Dong, C. (2015). Trapped lipopolysaccharide and LptD intermediates reveal lipopolysaccharide translocation steps across the *Escherichia coli* outer membrane. *Scientific Reports*, 5, 11883.
- Li, Y., Orlando, B. J., & Liao, M. (2019). Structural basis of lipopolysaccharide extraction by the LptB<sub>2</sub>FG complex. *Nature*, 567, 486–490.
- Lo Sciuto, A., Martorana, A. M., Fernández-Piñar, R., Mancone, C., Polissi, A., & Imperi, F. (2018). *Pseudomonas aeruginosa* LptE is crucial for LptD assembly, cell envelope integrity, antibiotic resistance and virulence. *Virulence*, 9, 1718–1733.
- Luo, Q., Yang, X., Yu, S., Shi, H., Wang, K., Xiao, L., Zhu, G., Sun, C., Li, T., Li, D., et al. (2017). Structural basis for lipopolysaccharide extraction by ABC transporter LptB<sub>2</sub>FG. *Nature Structural & Molecular Biology*, 24, 469–474.
- Ma, B., Fang, C., Lu, L., Wang, M., Xue, X., Zhou, Y., Li, M., Hu, Y., Luo, X., & Hou, Z. (2019). The antimicrobial peptide thanatin disrupts the bacterial outer membrane and inactivates the NDM-1 metallo- $\beta$ -lactamase. *Nature Communications*, 10, 3517.
- MacNair, C. R., Tsai, C. N., & Brown, E. D. (2020). Creative targeting of the Gram-negative outer membrane in antibiotic discovery. *Annals of the New York Academy of Sciences*, 1459, 69–85.
- Magill, S. S., Edwards, J. R., Bamberg, W., Beldavs, Z. G., Dumyati, G., Kainer, M. A., Lynfield, R., Maloney, M., McAllister-Holod, L., Nadle, J., et al. (2014). Multistate point-prevalence survey of health care-associated infections. *The New England Journal of Medicine*, 370, 1198–1208.
- Malojčić, G., Andres, D., Grabowicz, M., George, A. H., Ruiz, N., Silhavy, T. J., & Kahne, D. (2014). LptE binds to and alters the physical state of LPS to catalyze its assembly at the cell surface. *Proceedings of the National Academy of Sciences of the United States of America*, 111, 9467–9472.
- Mandler, M. D., Baidin, V., Lee, J., Pahl, K. S., Owens, T. W., & Kahne, D. (2018). Novobiocin enhances polymyxin activity by stimulating lipopolysaccharide transport. *Journal of the American Chemical Society*, 140, 6749–6753.
- Martín-Loeches, I., Dale, G. E., & Torres, A. (2018). Murepavadin: A new antibiotic class in the pipeline. *Expert Review of Anti-Infective Therapy*, 16, 259–268.
- Martorana, A. M., Sperandio, P., Polissi, A., & Dehò, G. (2011). Complex transcriptional organization regulates an *Escherichia coli*

- locus implicated in lipopolysaccharide biogenesis. *Research in Microbiology*, 162, 470–482.
- May, J. M., Owens, T. W., Mandler, M. D., Simpson, B. W., Lazarus, M. B., Sherman, D. J., Davis, R. M., Okuda, S., Massefski, W., Ruiz, N., et al. (2017). The antibiotic novobiocin binds and activates the ATPase that powers lipopolysaccharide transport. *Journal of the American Chemical Society*, 139, 17221–17224.
- Melchers, M. J., Teague, J., Warn, P., Hansen, J., Bernardini, F., Wach, A., Obrecht, D., Dale, G. E., & Mouton, J. W. (2019). Pharmacokinetics and pharmacodynamics of murepavadin in neutropenic mouse models. *Antimicrobial Agents and Chemotherapy*, 63, e01699–e1718.
- Mi, W., Li, Y., Yoon, S. H., Ernst, R. K., Walz, T., & Liao, M. (2017). Structural basis of MsbA-mediated lipopolysaccharide transport. *Nature*, 549, 233–237.
- Moffatt, J. H., Harper, M., Harrison, P., Hale, J. D., Vinogradov, E., Seemann, T., Henry, R., Crane, B., St Michael, F., Cox, A. D., et al. (2010). Colistin resistance in *Acinetobacter baumannii* is mediated by complete loss of lipopolysaccharide production. *Antimicrobial Agents and Chemotherapy*, 54, 4971–4977.
- Moura, E. C. C. M., Baeta, T., Romanelli, A., Laguri, C., Martorana, A. M., Erba, E., Simorre, J., Sperandio, P., & Polissi, A. (2020). Thanatin impairs lipopolysaccharide transport complex assembly by targeting LptC–LptA interaction and decreasing LptA stability. *Frontiers in Microbiology*, 11, 909.
- Narita, S., & Tokuda, H. (2009). Biochemical characterization of an ABC transporter LptBFGC complex required for the outer membrane sorting of lipopolysaccharides. *FEBS Letters*, 583, 2160–2164.
- Okuda, S., Freinkman, E., & Kahne, D. (2012). Cytoplasmic ATP hydrolysis powers transport of lipopolysaccharide across the periplasm in *E. coli*. *Science*, 338, 1214–1217.
- Okuda, S., Sherman, D. J., Silhavy, T. J., Ruiz, N., & Kahne, D. (2016). Lipopolysaccharide transport and assembly at the outer membrane: The PEZ model. *Nature Reviews Microbiology*, 14, 337–345.
- Owens, T. W., Taylor, R. J., Pahil, K. S., Bertani, B. R., Ruiz, N., Kruse, A. C., & Kahne, D. (2019). Structural basis of unidirectional export of lipopolysaccharide to the cell surface. *Nature*, 567, 550–553.
- Pahil, K. S., Gilman, M. S. A., Baidin, V., Clairfeuille, T., Mattei, P., Bieniossek, C., Dey, F., Muri, D., Baettig, R., Lobritz, M., et al. (2024). A new antibiotic traps lipopolysaccharide in its intermembrane transporter. *Nature*, 625, 572–577.
- Peng, D., Hong, W., Choudhury, B. P., Carlson, R. W., & Gu, X. (2005). *Moraxella catarrhalis* bacterium without endotoxin, a potential vaccine candidate. *Infection and Immunity*, 73, 7569–7577.
- Prasad, N. K., Seiple, I. B., Cirz, R. T., & Rosenberg, O. S. (2022). Leaks in the pipeline: A failure analysis of Gram-negative antibiotic development from 2010 to 2020. *Antimicrobial Agents and Chemotherapy*, 66, e0005422.
- Qiao, S., Luo, Q., Zhao, Y., Zhang, X. C., & Huang, Y. (2014). Structural basis for lipopolysaccharide insertion in the bacterial outer membrane. *Nature*, 511, 108–111.
- Raetz, C. R. H., & Whitfield, C. (2002). Lipopolysaccharide endotoxins. *Annual Review of Biochemistry*, 71, 635–700.
- Raetz, C. R. H., Reynolds, C. M., Trent, M. S., & Bishop, R. E. (2007). Lipid A modification systems in Gram-negative bacteria. *Annual Review of Biochemistry*, 76, 295–329.
- Robinson, J. A., Shankaramma, S. C., Jetter, P., Kienzl, U., Schwendener, R. A., Vrijbloed, J. W., & Obrecht, D. (2005). Properties and structure–activity studies of cyclic  $\beta$ -hairpin peptidomimetics based on the cationic antimicrobial peptide protegrin I. *Bioorganic & Medicinal Chemistry*, 13, 2055–2064.
- Romano, K. P., & Hung, D. T. (2023). Targeting LPS biosynthesis and transport in Gram-negative bacteria in the era of multi-drug resistance. *Biochimica et Biophysica Acta (BBA) Molecular Cell Research*, 1870, 119407.
- Ruiz, N., Gronenberg, L. S., Kahne, D., & Silhavy, T. J. (2008). Identification of two inner-membrane proteins required for the transport of lipopolysaccharide to the outer membrane of *Escherichia coli*. *Proceedings of the National Academy of Sciences of the United States of America*, 105, 5537–5542.
- Ruiz, N., Chng, S., Hiniker, A., Kahne, D., & Silhavy, T. J. (2010). Nonconsecutive disulfide bond formation in an essential integral outer membrane protein. *Proceedings of the National Academy of Sciences of the United States of America*, 107, 12245–12250.
- Sabnis, A., & Edwards, A. M. (2023). Lipopolysaccharide as an antibiotic target. *Biochimica et Biophysica Acta BBA Molecular Cell Research*, 1870, 119507.
- Sader, H. S., Dale, G. E., Rhomberg, P. R., & Flamm, R. K. (2018). Antimicrobial activity of murepavadin tested against clinical isolates of *Pseudomonas aeruginosa* from the United States, Europe, and China. *Antimicrobial Agents and Chemotherapy*, 62, e00311–e318.
- Santambrogio, C., Sperandio, P., Villa, R., Sobott, F., Polissi, A., & Grandori, R. (2013). LptA assembles into rod-like oligomers involving disorder-to-order transitions. *Journal of the American Society for Mass Spectrometry*, 24, 1593–1602.
- Schmidt, J., Patora-Komisarska, K., Moehle, K., Obrecht, D., & Robinson, J. A. (2013). Structural studies of  $\beta$ -hairpin peptidomimetic antibiotics that target LptD in *Pseudomonas* sp. *Bioorganic & Medicinal Chemistry*, 21, 5806–5810.
- Schultz, K. M., Feix, J. B., & Klug, C. S. (2013). Disruption of LptA oligomerization and affinity of the LptA–LptC interaction. *Protein Science*, 22, 1639–1645.
- Schultz, K. M., Lundquist, T. J., & Klug, C. S. (2017). Lipopolysaccharide binding to the periplasmic protein LptA. *Protein Science*, 26, 1517–1523.
- Schuster, M., Brabet, E., Oi, K. K., Desjonquères, N., Moehle, K., Le Poupon, K., Hell, S., Gable, S., Rithié, V., Dillinger, S., et al. (2023). Peptidomimetic antibiotics disrupt the lipopolysaccharide transport bridge of drug-resistant Enterobacteriaceae. *Science Advances*, 9, eadg3683.
- Sestito, S. E., Sperandio, P., Santambrogio, C., Ciaramelli, C., Calabrese, V., Rovati, G. E., Zambelloni, L., Grandori, R., Polissi, A., & Peri, F. (2014). Functional characterization of *E. coli* LptC: Interaction with LPS and a synthetic ligand. *ChemBioChem*, 15, 734–742.
- Shankaramma, S. C., Moehle, K., James, S., Vrijbloed, J. W., Obrecht, D., & Robinson, J. A. (2003). A family of macrocyclic antibiotics with a mixed peptide–peptoid  $\beta$ -hairpin backbone conformation. *Chemical Communications*, 15, 1842–1843.
- Sherman, D. J., Okuda, S., Denny, W. A., & Kahne, D. (2013). Validation of inhibitors of an ABC transporter required to transport lipopolysaccharide to the cell surface in *Escherichia coli*. *Bioorganic & Medicinal Chemistry*, 21, 4846–4851.
- Sherman, D. J., Lazarus, M. B., Murphy, L., Liu, C., Walker, S., Ruiz, N., & Kahne, D. (2014). Decoupling catalytic activity from biological function of the ATPase that powers lipopolysaccharide transport. *Proceedings of the National Academy of Sciences of the United States of America*, 111, 4982–4987.
- Sherman, D. J., Xie, R., Taylor, R. J., George, A. H., Okuda, S., Foster, P. J., Needleman, D. J., & Kahne, D. (2018). Lipopolysaccharide is transported to the cell surface by a membrane-to-membrane protein bridge. *Science*, 359, 798–801.
- Silver, L. L. (2011). Challenges of antibacterial discovery. *Clinical Microbiology Reviews*, 24, 71–109.
- Simpson, B. W., Owens, T. W., Orabella, M. J., Davis, R. M., May, J. M., Trauger, S. A., Kahne, D., & Ruiz, N. (2016). Identification



- of residues in the lipopolysaccharide ABC transporter that coordinate ATPase activity with extractor function. *mBio*, 7, e01729-16.
- Sinha, S., Dhanabal, V. B., Sperandio, P., Polissi, A., & Bhattacharjya, S. (2022). Linking dual mode of action of host defense antimicrobial peptide thanatin: structures, lipopolysaccharide and LptA<sub>m</sub> binding of designed analogs. *Biochimica et Biophysica Acta (BBA) Biomembranes*, 1864, 183839.
- Sperandio, P., Cescutti, R., Villa, R., Di Benedetto, C., Candia, D., Dehò, G., & Polissi, A. (2007). Characterization of *lptA* and *lptB*, two essential genes implicated in lipopolysaccharide transport to the outer membrane of *Escherichia coli*. *Journal of Bacteriology*, 189, 244–253.
- Sperandio, P., Villa, R., Martorana, A. M., Šamalikova, M., Grandori, R., Dehò, G., & Polissi, A. (2011). New insights into the Lpt machinery for lipopolysaccharide transport to the cell surface: LptA-LptC interaction and LptA stability as sensors of a properly assembled transenvelope complex. *Journal of Bacteriology*, 193, 1042–1053.
- Srinivas, N., Jetter, P., Ueberbacher, B. J., Werneburg, M., Zerbe, K., Steinmann, J., Van der Meijden, B., Bernardini, F., Lederer, A., Dias, R. L., et al. (2010). Peptidomimetic antibiotics target outer-membrane biogenesis in *Pseudomonas aeruginosa*. *Science*, 327, 1010–1013.
- Steeghs, L., De Cock, H., Evers, E., Zomer, B., Tommassen, J., & Van Der Ley, P. (2001). Outer membrane composition of a lipopolysaccharide-deficient *Neisseria meningitidis* mutant. *The EMBO Journal*, 20, 6937–6945.
- Suits, M. D. L., Sperandio, P., Dehò, G., Polissi, A., & Jia, Z. (2008). Novel structure of the conserved Gram-negative lipopolysaccharide transport protein A and mutagenesis analysis. *Journal of Molecular Biology*, 380, 476–488.
- Sun, J., Rutherford, S. T., Silhavy, T. J., & Huang, K. C. (2021). Physical properties of the bacterial outer membrane. *Nature Reviews Microbiology*, 20, 236–248.
- Tang, X., Chang, S., Luo, Q., Zhang, Z., Qiao, W., Xu, C., Zhang, C., Niu, Y., Yang, W., Wang, T., et al. (2019). Cryo-EM structures of lipopolysaccharide transporter LptB<sub>2</sub>FGC in lipopolysaccharide or AMP-PNP-bound states reveal its transport mechanism. *Nature Communications*, 10, 4175.
- Tefsen, B., Geurtsen, J., Beckers, F., Tommassen, J., & De Cock, H. (2005). Lipopolysaccharide transport to the bacterial outer membrane in spheroplasts. *Journal of Biological Chemistry*, 280, 4504–4509.
- Theuretzbacher, U., Baraldi, E., Ciabuschi, F., & Callegari, S. (2023). Challenges and shortcomings of antibacterial discovery projects. *Clinical Microbiology and Infection*, 29, 610–615.
- Törk, L., Moffatt, C. B., Bernhardt, T. G., Garner, E. C., & Kahne, D. (2023). Single-molecule dynamics show a transient lipopolysaccharide transport bridge. *Nature*, 623, 814–819.
- Tran, A. X., Dong, C., & Whitfield, C. (2010). Structure and functional analysis of LptC, a conserved membrane protein involved in the lipopolysaccharide export pathway in *Escherichia coli*. *Journal of Biological Chemistry*, 285, 33529–33539.
- Upert, G., Luther, A., Obrecht, D., & Ermert, P. (2021). Emerging peptide antibiotics with therapeutic potential. *Medicine in Drug Discovery*, 9, 100078.
- Vetterli, S. U., Zerbe, K., Müller, M., Urfer, M., Mondal, M., Wang, S. Y., Moehle, K., Zerbe, O., Vitale, A., Pessi, G., et al. (2018). Thanatin targets the intermembrane protein complex required for lipopolysaccharide transport in *Escherichia coli*. *Science Advances*, 4, eaau2634.
- Villa, R., Martorana, A. M., Okuda, S., Gourlay, L. J., Nardini, M., Sperandio, P., Dehò, G., Bolognesi, M., Kahne, D., & Polissi, A. (2013). The *Escherichia coli* Lpt transenvelope protein complex for lipopolysaccharide export is assembled via conserved structurally homologous domains. *Journal of Bacteriology*, 195, 1100–1108.
- Wach, A., Dembowski, K., & Dale, G. E. (2018). Pharmacokinetics and safety of intravenous murepavadin infusion in healthy adult subjects administered single and multiple ascending doses. *Antimicrobial Agents and Chemotherapy*, 62, e02355-e2417.
- Wang, Z., Xiang, Q., Zhu, X., Dong, H., He, C., Wang, H., Zhang, Y., Wang, W., & Dong, C. (2014). Structural and functional studies of conserved nucleotide-binding protein LptB in lipopolysaccharide transport. *Biochemical and Biophysical Research Communications*, 452, 443–449.
- Willyard, C. (2017). The drug-resistant bacteria that pose the greatest health threats. *Nature*, 543, 15.
- Wilson, A. L., & Ruiz, N. (2022). The transmembrane  $\alpha$ -helix of LptC participates in LPS extraction by the LptB<sub>2</sub>FGC transporter. *Molecular Microbiology*, 118, 61–76.
- Wu, T., Malinverni, J., Ruiz, N., Kim, S., Silhavy, T. J., & Kahne, D. (2005). Identification of a multicomponent complex required for outer membrane biogenesis in *Escherichia coli*. *Cell*, 121, 235–245.
- Wu, T., McCandlish, A. C., Gronenberg, L. S., Chng, S., Silhavy, T. J., & Kahne, D. (2006). Identification of a protein complex that assembles lipopolysaccharide in the outer membrane of *Escherichia coli*. *Proceedings of the National Academy of Sciences of the United States of America*, 103, 11754–11759.
- Yang, Y., Chen, H., Corey, R. A., Morales, V., Quentin, Y., Froment, C., Caumont-Sarcos, A., Albenne, C., Burlet-Schiltz, O., Ranava, D., et al. (2023). LptM promotes oxidative maturation of the lipopolysaccharide translocon by substrate binding mimicry. *Nature Communications*, 14, 6368.
- Zampaloni, C., Mattei, P., Bleicher, K., Winther, L., Thäte, C., Bucher, C., Adam, J. M., Alanine, A., Amrein, K. E., Baidin, V., et al. (2024). A novel antibiotic class targeting the lipopolysaccharide transporter. *Nature*, 625, 566–571.
- Zhang, Q., Lambert, G., Liao, D., Kim, H., Robin, K., Tung, C., Pourmand, N., & Austin, R. H. (2011). Acceleration of emergence of bacterial antibiotic resistance in connected microenvironments. *Science*, 333, 1764–1767.
- Zhang, G., Meredith, T. C., & Kahne, D. (2013). On the essentiality of lipopolysaccharide to Gram-negative bacteria. *Current Opinion in Microbiology*, 16, 779–785.
- Zhang, G., Baidin, V., Pahil, K. S., Moison, E., Tomasek, D., Ramadoss, N. S., Chatterjee, A. K., McNamara, C. W., Young, T. S., Schultz, P. G., et al. (2018). Cell-based screen for discovering lipopolysaccharide biogenesis inhibitors. *Proceedings of the National Academy of Sciences of the United States of America*, 115, 6834–6839.
- Zhang, X., Li, Y., Wang, W., Zhang, J., Lin, Y., Hong, B., You, X., Song, D., Wang, Y., Jiang, J., et al. (2019). Identification of an anti-Gram-negative bacteria agent disrupting the interaction between lipopolysaccharide transporters LptA and LptC. *International Journal of Antimicrobial Agents*, 53, 442–448.
- Zhou, P., & Zhao, J. (2017). Structure, inhibition, and regulation of essential lipid A enzymes. *Biochimica et Biophysica Acta BBA Molecular and Cell Biology of Lipids*, 1862, 1424–1438.
- Zietek, M., Miguel, A., Khusainov, I., Shi, H., Asmar, A. T., Ram, S., Wartel, M., Sueki, A., Schorb, M., Goulian, M., et al. (2022). Bacterial cell widening alters periplasmic size and activates envelope stress responses. *bioRxiv*, <https://doi.org/10.1101/2022.07.26.501644>.

Springer Nature or its licensor (e.g. a society or other partner) holds exclusive rights to this article under a publishing agreement with the author(s) or other rightsholder(s); author self-archiving of the accepted manuscript version of this article is solely governed by the terms of such publishing agreement and applicable law.